Transworld Research Network
37/661 (2), Fort P.O., Trivandrum-695 023, Kerala, India


Recent Res. Devel. Biophys., 3(2004): 61-86 ISBN: 81-7895-130-4

# 4 The birth, life and death of statistical pores into a bilayer membrane

**Liviu Movileanu[1,2] and Dumitru Popescu[3,4]**
[1]Department of Physics, Syracuse University, College of Arts and Sciences, 201 Physics Building, Syracuse, New York 13244-1130, USA; [2]Structural Biology Biochemistry and Biophysics Program (SB3), Syracuse University, 111 College Place Syracuse, New York 13244-4100, USA; [3]Laboratory of Biophysics, University of Bucharest, Faculty of Biology, Splaiul Independentei 91–95, Bucharest R–76201 Romania; [4]Institute of Applied Mathematics, Calea 13 Septembrie 13, P.O.Box 1–24 Bucharest, Romania

## Abstract

*There is a significant evidence indicating that pores of nanoscopic dimensions can stochastically form and grow in a lipid bilayer of a cell membrane following an activated process induced by an external trigger such as thermal fluctuations, transmembrane electrical potential, mechanical stress or other changes in the cellular environment. In this review article, we present an overview of recent theoretical and experimental developments to better understand the mechanisms responsible for stochastic pore*

Correspondence/Reprint request: Dr. Liviu Movileanu, Laboratory of Single-Molecule Biophysics, Syracuse University Department of Physics, 201 Physics Building, Syracuse NY 13244-1130, USA. E-mail: movileanu@physics.syr.edu

*formation. A transient pore may open or close, thus the final pore state and its kinetics are dependent on the forces that act on the pore boundary. These are: (1) the surface tension, which reduces the free energy barrier for pore formation, and (2) line tension, which increases the free energy barrier for pore formation.The recent results regarding the kinetics of pore opening and resealing are also discussed. The pore formation in a membrane has multiple projected applications including drug delivery and gene therapy. Several experimental strategies were examined, such as the use of a suitable chemical agent, pore-forming peptides, electroporation, temperature jump or osmotic shock to bring about an increase in membrane permeability for DNA or drug molecules.*

# 1. Introduction

The lipid bilayer of the cell membranes is a remarkable self-assembled, complex and fluctuating structure that undergoes to a variety of conformational and nonequilibrium phase transitions, which are relevant to biological functions [1-3]. The bilayer fluctuations are extremely fast and involve subtle rearrangements at the single molecule level [4,5]. The formation of transient pores in membranes is an energetically favourable route for the transport of protons, water molecules and a diversity of hydrophilic compounds. Even a limited number of transmembrane hydrophilic pores can account for the experimentally determined rates for ion diffusion in the absence of translocation proteins [6,7]. Therefore, the bilayer lipid membranes (BLMs) are not perfectly insulating systems, but also permeable for water and different electrolytes that diffuse through transmembrane pores.

A transient pore in a bilayer membrane pore can form and grow because of a free energy-dependent activated process caused by an external trigger (e.g. a short duration and high amplitude electrical pulse) [8-13], random thermally induced fluctuations of the membrane phospholipids [14-17], and other changes of the cellular environment [18-22]. The physical properties of the transient pores depend on their formation mechanisms as well as the intensity of the external trigger (e.g. electrical pulse, temperature jump, osmotic shock etc.). For example, the radius of the pores can vary in a wide range from nanometer to micrometer scale. The pore lifetime is also dependent on both the intensity of the external trigger (e.g. osmotic shock, electric pulse etc.) and physical properties of the membrane (e.g.. bending, curvature, hydrophobicity, chain rigidity, compressibility etc.). The electroporated holes in membranes can last several microseconds, but the thermally induced unstable pores exhibit a much shorter lifetime in the order of several nanoseconds [17]. In an extreme situation, using micropipette extrusion on vesicles, Needham and Zhelev were able to demonstrate the presence of large transbilayer pores with a duration of a few seconds [23].

Majority of the models for pore formation in membranes are based on a simple hypothesis proposed three decades ago by Litster (1975) [24]. The appearance of a circular pore, of radius $r$, in a membrane with the surface tension coefficient $\gamma$, is balanced by the presence of two competing energetic terms: reduction in free energy barrier by the surface tension component $\pi r^2\gamma$, and increase in free energy barrier by a linear edge component $2\pi r\sigma$. The line tension ($\sigma$) is caused by the hydrophobic property of phospholipids, and contributes to the free energy barrier height against pore formation [25]. The surface tension $\gamma$ reduces this free energy barrier height for pore formation. Weaver and colleagues (1994) [8] have used such a model to interpret their electroporation experiments. The model accurately predicted that the pores with a size beyond a critical value evolve to an unstable structure such as that of rupture [16,18,26], whereas narrower pores undergo a resealing process [9,15,27]. On the other hand, the growth of thermally induced transbilayer pores was examined by Monte Carlo simulations in a two-dimensional fluid membrane model [14]. The simulations employed independent parameters for the pore formation such as line tension, surface tension and free energy barrier height for pore formation. For large line tensions, quasi-independent and narrow pores can be formed. In contrast, at low line tensions and high free energy barrier height, a single pore can be formed in an entropically driven phase transition.

# 2. Transbilayer pores induced by mechanical stress

We mentioned in the introduction of this review article that the pore formation, the pore lifetime as well as the pore closure (resealing) depend on the physical properties of the lipid bilayer. Among these, the membrane tension and pore line (edge) tension play a critical role for the membrane stability [28,29]. There is enough experimental evidence for the appearance of macroscopic pores in mechanically stretched vesicles [22,28,30, 31]. The interpretation on the control of the pore lifetime is largely based on the traditional model of Litster (1975) [24], which was mentioned above. The dynamics of the large pore size, in a micrometer scale, is given by the balance between two opposite contributions: pore growing, which is generated by the membrane surface tension, and pore shrinking, which is brought about by the line tension [30]. An exchange of water with a more viscous binary liquid mixture formed by water and glycerol permitted probing all the stages of pore kinetics: pore appearance, growth and closure. A leak-out of the hydrophobic layer occurs upon pore formation of large size, up to 10 μm, which favours a decrease in the surface tension [19,30,31]. This decrease in the surface tension ultimately induces the pore closure (see below). The binary liquid mixture is used to slow down the leak-out from the hydrophobic domain of the pore, thus permitting monitoring

the transbilayer pores in a second timescale. The immersion of the vesicles in a highly viscous medium sufficed the visualization of the pores by stretching out the membranes either via intense illumination or via their adhesion on a solid support. If the solution is of low viscosity (e.g. water), a leak-out is quite fast. Therefore, the pore closes before attaining a large and visible size, so that the pore lifetime is quite short. The transient pores in mechanically stretched giant vesicles were visualized with an upright fluorescence microscope [31]. The pores measured a diameter larger than a critical value $d_{c1}$. The pores grew up to a second value $d_{c2}$, after which they closed. Upper limit $d_{c2}$ was explained by relaxation process of the surface tension, as the holes increase in size. The pore closure was interpreted as a subsequent relaxation of the line tension upon the exit of the internal liquid. In other words, the line tension of the pore boundary is able to drive a resealing of the transient pore. Karatekin and co-workers (2003) [22] were able to accurately derive the line tension ($\sigma$) from the resealing velocity of the pores. The effect of inclusion molecules within the lipid bilayers was examined. Thus, they found that cholesterol, as modelled like an inverted cone-shaped molecule, promotes an increase in the line tension. In contrast, the presence of some cone-shaped detergents within membrane environment reduced the line tension. Very surprisingly, this effect could rise the transient pore lifetime up to several minutes!

Other groups have been able to visualize long-lived and wide holes in membranes by electroporation combined with a large membrane tension induced my micropipette aspiration [19,23]. Moroz and Nelson (1997) [19] explained the surprising lifetime of the pores by a feedback mechanism that regulates the stability of the transient transmembrane pores. The feedback is a result of the balance between the solution flowing through the pore and the velocity of the vesicles's leading boundary while it is aspirated into the pipette. This contributes substantially to a decrease in surface tension, which is given by two distinct parameters: the pore radius and projected length of the membrane in the pipette. The physical formalism used for this type of experiments permitted an accurate determination of the line tension of the bilayer membrane. Influence of the mechanical stress on the fluid lipid bilayers was pursued by Shillcock and Boal [18,32]. The model parameters were the stress applied to the membrane and the edge tension of the pore. Interestingly enough, at zero stress and large edge tension, the narrow pores are present within the membrane, which may be consistent with the statistical fluctuations of the membrane. A phase diagram for the membrane stability was inferred using this model, in which the compression balancing the edge tension can give rise to multiple stability-instability domains with open and closed pores.

# 3. Thermally induced thickness fluctuations, membrane elasticity and pore formation

## 3.1. Why do thickness fluctuations produce transbilayer pores?

The BLM hydrophobic thickness fluctuations was experimentally [33] as well as theoretically [34,35] evidenced. For a mixture of lipids in BLMs, a selective association between phospholipids can generate phospholipid domains and local changes in hydrophobic thickness [36]. The phospholipid domain thickness is strongly dependent on the length of the hydrocarbon chain of phospholipids [37-42]. The appearance of a transient stochastic pore in a lipid membrane due to thickness fluctuations was first demonstrated by Popescu and co-workers [29]. The energy barrier height for membrane local rupture following such a mechanism is quite large (~ 91 $k_BT$) [29], where $k_B$ and $T$ have their usual meaning. In this case, the geometrical profile of the pore is an elliptical one (Fig. 1). It was also shown that such a transmembrane pore could evolve to a stable state, which was unexpected because of the rapid timescale for resealing of statistical pores in membranes. In agreement with this theoretical prediction, Zhelev and Needham (1993) [23] have created large and quasi-stable pores in lipid bilayer vesicles [29].

We recently proposed a model for the appearance of either transient or stable transbilayer pores of nanoscopic dimension via elastic fluctuations of the membrane thickness [27] (Fig. 2). We implemented the elasticity theory of continuous media [27,43-47] to study the appearance of stochastic pores in a lipid membrane. A planar membrane conformation that is stable at zero temperature can become highly unstable at higher temperatures. We have examined the conditions for transbilayer pore formation brought about by membrane thickness fluctuations. The pore radius was estimated assuming that the BLM deformation free energy is equal to the total thermal energy of the phospholipids that co-participate to the collective thermal motion (CTM). Thus, we applied the elastic theory of continuous media to calculate the bilayer deformation free energy necessary to create a single transbilayer pore. In lipid bilayers with a thick hydrophobic layer ($2h > 28$ Å), two iso-energetic pores (the same free energy barrier for pore formation) with distinct geometrical configurations can occur. The polar headgroup size has a strong influence on the phenomenon of transmembrane pore formation (see below). Large polar headgroups can produce bilayer rupture brought about by thermoporation.

From a structural point of view, lateral translations with random directions induce local fluctuations of the density of the lipid polar headgroups at BLM surfaces [13,17,48]. Therefore, a snapshot of the BLM surface reveals local domains of nanoscopic dimension with a higher density of polar headgroups (called also as clusters) as well as zones with a lower density. These defects may disappear or propagate within the core of the lipid bilayer.

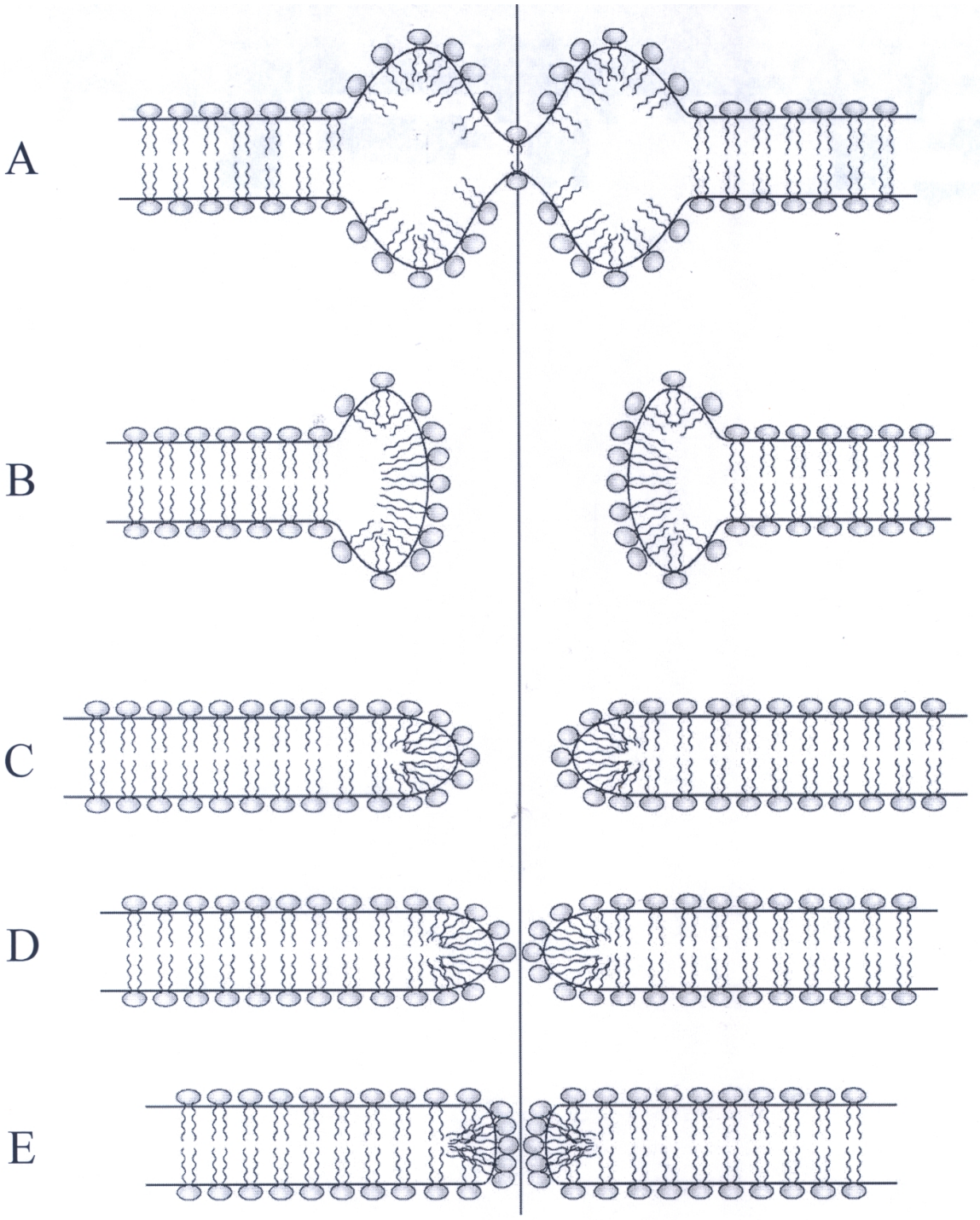


**Figure 1.** The hypothesized kinetics of the formation, stabilization, and closure of the stochastic transbilayer pores. (A) The oscillation state of the lipid bilayer accompanied by thickness fluctuations; (B) Perforation of the lipid bilayer that is caused by thickness fluctuations; (C) The state of stabilized pore; (D) Fluctuations in surface tension or thickness fluctuations in the proximity of the pore can induce the pore closure; (E) The transbilayer pore is closed like a zipper.

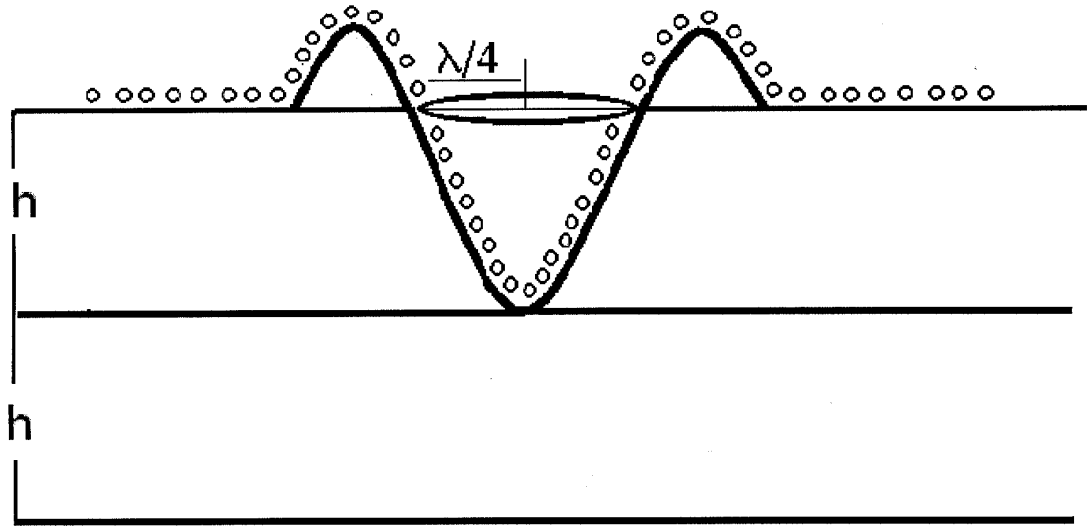


**Figure 2.** Thermally induced undulation of the lipid bilayer: $\lambda$ and $h$ are the BLM deformation wavelength and the half-thickness of the hydrophobic core, respectively.

Thermal movement of a lipid molecule perpendicularly oriented on the bilayer surface influences the motion of neighboring molecules due to intermolecular forces. We can assume that the molecular interaction forces determine a group of molecules to move from one surface towards the other, in the same direction, with some a certain delay between them. This collection of molecules participates to a thermally induced group motion and constitutes the perturbing factor that produces a local thinning of the BLM hydrophobic thickness. This process is known as the thermally induced membrane undulation. Thermally induced undulations overlap over these structural thickness fluctuations. It is possible for the deformation of one monolayer to overlap with the deformation of the other monolayer, and the amplitudes of both deformations can be equal to half the bilayer thickness. In this situation, the lipid bilayer breakdown can produce pores generated by fluctuations in thickness, thus determined by thermally induced movements of lipid molecules perpendicularly oriented to the bilayer surface.

## 3.2. The bilayer deformation energy

Lipid bilayers exhibit behavior of liquid crystals smectic of type A with parallel layers [45,46]. The molecules of the two individual layers have their axes perpendicularly oriented on the layer interfaces. Therefore, the calculus of energy for a pore birth is equivalent to the calculus of deformation free energy of the lipid bilayer, provided that the deformation amplitude is equal to the hydrophobic half-thickness. According to the elasticity theory of continuum media applied to smectic liquid crystals of type A, the variation of free energy per unit surface is given by [27,45,46,49,50]:

$$\Delta F(x,y) = h\bar{B}\left(\frac{u}{h}\right)^2 + hK_1\left(\frac{\partial^2 u}{\partial x^2} + \frac{\partial^2 u}{\partial y^2}\right)^2 + \gamma\left[\left(\frac{\partial u}{\partial x}\right)^2 + \left(\frac{\partial u}{\partial y}\right)^2\right] \quad (1)$$

where $u(x,y)$ represents the surface displacement with respect to its initial position, when the surface is planar and $h$ is the half-thickness of the hydrophobic core of lipid bilayer.

In formula (1) there are three terms. The first one represents the variation in free energy due to lipid bilayer compression, characterized by the elasticity coefficient $\bar{B}$ [47]. The second term indicates the variation in free energy due to position displacements of molecular axes with respect to their initial position, perpendicularly oriented to the lipid bilayer surface. This is characterized by the elastic splay constant $K_1$. In formula (1) we consider only marginal and slow variations in molecular axis that co-participate to the deformation. The third term is the variation in free energy determined by the change of bilayer surface that was generated by deformation. This term is characterized by the surface tension coefficient $\gamma$. Taking into account that the deformation has cylindrical symmetry

$$\Delta F(r) = \bar{B}\frac{u^2}{h} + hK_1\left(\frac{\partial u}{r\partial r} + \frac{\partial^2 u}{\partial r^2}\right)^2 + \gamma\left(\frac{\partial u}{\partial r}\right)^2 \quad (2)$$

Considering that any deformation can be decomposed into unit sine-shaped deformations $u(r,\lambda)$ (Figs. 2,3) is given by the following form:

$$u(r,\lambda) = \pm h\cos\frac{2\pi r}{\lambda} \quad (3)$$

The hydrophobic core thickness is $2h$, and $\lambda$ is the BLM deformation wavelength (Figs. 2,3).

## 3.3. Conditions of pore appearance

The initial state of the BLM was considered that in which the molecules do not exhibit movements (i.e. we consider a zero initial temperature). At this temperature, both surfaces of the BLM are planar. By warming the BLM up to temperatures $T > 0$ K, the phospholipids get kinetic energies and their thermal motions will start deforming the lipid bilayer. This phenomenon induces the appearance of thickness fluctuations [29,51]. Thus, this thermal energy must be equal or greater than the BLM deformation free energy:

$$\frac{a_0}{\pi R^2}\Delta\overline{F} \le (3N - N_b)\frac{kT}{2} \tag{4}$$

where $a_0$ represents the cross–sectional area of the polar headgroups [52], $R$ is the radius of the region of collective thermal motion (CTM), $N$ is the number of atoms of a single molecule, $N_b$ is the number of chemical intra–molecular bonds, $k$ and $T$ have their usual meanings.

We are interested to find the parameters $\lambda$ and $R$ that satisfy the following relation:

$$\frac{2a_0}{R^2}\int_0^R rF(r,\lambda)dr = (3N - N_b)\frac{kT}{2} \tag{5}$$

For a polyatomic molecule, we have $3N - N_b = 6$

After some calculus, the last equation can be written as:

$$a(y)x^4 + b(y)x^2 + c(y) = 0 \tag{6}$$

where the dimensionless variables $x$ and $y$ and the functions $a(y)$ , $b(y)$ , $c(y)$ are given by the following expression:

$$\begin{aligned}
&x = h\frac{2\pi}{\lambda},\ y = R\frac{2\pi}{\lambda}\\
&a(y) = \frac{K_1}{\overline{B}h^2}\left(1 + \frac{\sin 2y}{y} - 3\frac{\cos 2y - 1}{2y^2} + \frac{4}{y^2}\int_0^1 \frac{\sin^2 ty}{t}dt\right)\\
&b(y) = \frac{\gamma}{\overline{B}h}\left(1 - \frac{\sin 2y}{y} - \frac{\cos 2y - 1}{2y^2}\right)\\
&c(y) = 1 + \frac{\sin 2y}{y} + \frac{\cos 2y - 1}{2y^2} - (3N - N_b)\frac{kT}{\overline{B}ha_0}
\end{aligned} \tag{7}$$

Unfortunately the Eq. 6 is very complex to allow obtaining the explicit formulae for $\lambda$ and $R$, but one can obtain their parametrical representations. Eq. 6 is an algebraic one for $x$ as a function of parameter $y$. Since the functions $a$ and $b$ are always positive, the equation has real solutions only if the function $c$ is negative. With these conditions, we are able to get a single positive solution of Eq. 6:

$$\begin{aligned}
&\lambda(y) = 2\pi h\left(\sqrt{\frac{2a(y)}{-b(y) + \sqrt{b^2(y) - 4a(y)c(y)}}}\right)\\
&R(y) = \frac{y\lambda(y)}{2\pi}
\end{aligned} \tag{8}$$

Using Eq.6, we have determined $R$ and $\lambda$ values for which thermal group motion determines a local deformation of amplitude $h$, which can result in lipid bilayer perforation. It is worth mentioning that the wavelength $\lambda$ depends on the interactions between the polar headgroups and the relative motions of the neighboured molecules. In other words, the BLM deformation wavelength depends on the dephasing that appears between the neighboured molecules along the radius of the BLM surface occupied by the molecules involved in the CTM.

## 3.4. Pore radius calculus

After BLM rupture, a rearrangement of molecules located in the deformation domain takes place, so that the surface of the sinusoidal toroid modifies its concavity becoming a surface of a revolution elliptic toroid. By equating the volumes delimited by the two revolution surfaces (i.e. sinusoidal and ellipsoidal), both before the BLM rupture and after molecular rearrangement, the pore radius can be calculated. In the next steps, we calculate these two volumes.

We consider the space domain, D, of an ellipsoidal toroid, defined by the relations (Fig. 3):

$$z \in (0,h),\ r \le \lambda/4$$
$$\frac{z^2}{h^2} + \frac{(r-\lambda/4)^2}{b^2} \le 1 \qquad (9)$$

where $b$ is a parameter that fixes the space configuration of the pore.

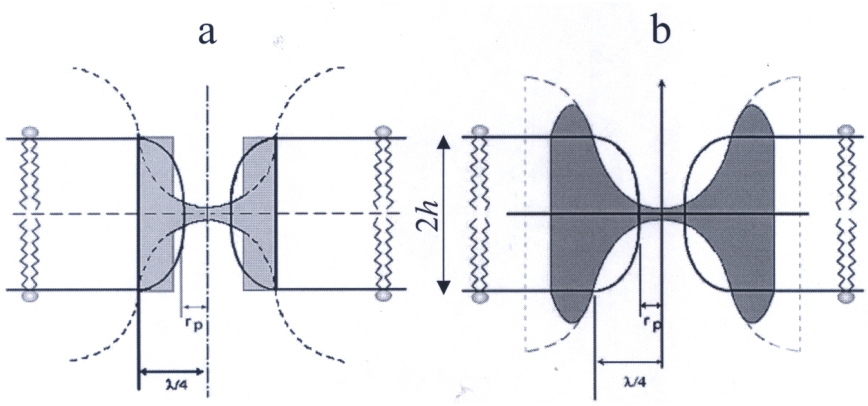


**Figure 3.** Cross-sectional view through the BLM deformed in the case in which the radius, $R$, of the perturbation zone is: a) lower than $\lambda/4$, and b) larger than $\lambda/4$. $\lambda$ and $r_p$ indicate the BLM deformation wavelength and the radius of the pore, respectively. The lipid rearrangement starts just immediately after the BLM perforation. The molecules, which belonged to the volume represented in section by hatched region in this figure before the membrane perforation, will be found in the volume limited by the elliptical surface of toroid.

Using a system of polar coordinates, the volume $D$ of an ellipsoidal toroid is given by:

$$V = 2\pi \iint_D r dr dz \tag{10}$$

With some calculations, one can obtain the expression for $V$:

$$V_a(\lambda, b) = 2\pi h \begin{cases} b\left(\frac{\lambda\pi}{16} - \frac{b}{3}\right), & b \le \frac{\lambda}{4} \\ \frac{\lambda^2}{32}\sqrt{1-\left(\frac{\lambda}{4b}\right)^2} + \frac{\lambda b}{8}\arcsin\frac{\lambda}{4b} + \frac{b^2}{3}\left[\left(\sqrt{1-\left(\frac{\lambda}{4b}\right)^2}\right)^3 - 1\right], & b \ge \frac{\lambda}{4} \end{cases} \tag{11}$$

The volume of the domain characterising a sinusoidal toroid is given by:

$$V_l(\lambda, R) = 2\pi h\left(\frac{\lambda}{2\pi}\right)^2 \begin{cases} \frac{\pi^2}{8} + 1 - \cos\frac{2\pi R}{\lambda} - \frac{2\pi R}{\lambda}\sin\frac{2\pi R}{\lambda}, & R \le \frac{\lambda}{4} \\ \frac{\pi^2}{8} + 1 - \frac{\pi}{2} + \frac{4\pi R}{\lambda}\left(1 - \sin\frac{2\pi R}{\lambda}\right), & R \ge \frac{\lambda}{4} \end{cases} \tag{12}$$

Equating the two volumes given by the Eqs. (11) and (12), namely $V_a(\lambda, b)=V_l(\lambda, R)$, one can calculate the pore radius $r$. After rupture, molecules from the walls of the pore reorganize themselves into a stable membrane state having a pore inside.

The parameters of equation (1) can be divided in two categories, depending on their effect on the BLM deformation free energy change:

*i) direct parameters*, which characterize the interaction forces responsible for the bilayer energy change during deformation. These parameters are the elastic compression coefficient ( $\overline{B}$ ), the elastic splay coefficient ($K_1$) and the surface tension coefficient ($\gamma$).

(ii) *indirect parameters*, which are not directly related to the intermolecular interactions, and define the lipid bilayer state. These are the BLM hydrophobic core half-thickness ($h$), the cross-sectional area of phospholipids ($a_0$) and the absolute temperature ($T$). For phospholipids that self-assemble in planar lipid bilayers, the cross-sectional area $a_0$ is identical with the cross-section area of the polar headgroups or hydrophobic tails.

A very important and interesting result is the appearance of the most probable pore. The radius of this pore denoted with $r_{0p}$ corresponds to the lowest

value of $R$, denoted by $R_0$. The BLM deformation wavelength corresponding to $R_0$ is denoted by $\lambda_0$. Generally, the most probable pore is neither the largest nor the narrowest. It has the highest probability of appearance, because the number of phopsholipids that participate to the collective thermal movement (CTM) is the lowest. As a consequence, the BLM free energy change of is the lowest.

The lipid bilayers may be perforated only if the CTM cover a circular region on bilayer surface with a radius R belonging to a range noted as $[R_0, R_{max}]$ and called here the compatibility range with pore appearance, or simply compatibility range (CR). For all values of $R$ out of this range, the pore formation is not probable because the amplitude of bilayer deformation is less than hydrophobic core half-thickness ($h$).

Normally, the dependence of deformation wavelength, $\lambda$, is not a one-to-one function of $R$, but the pore radius $r_p$ is one-to-one function of . $\lambda$. So, the CR of $R$ will be divided in two sub-ranges: the noninjection range and the bijection range. For each value of $R$ from noninjectivity range, the Eq. 6 has two solutions for wavelength $\lambda$. However, for each value of $R$ from bijection range, the Eq. 6 has a single solution for $\lambda$. Because the pore radius is a one-to-one function of wavelength $\lambda$, it results that if the size of perturbation, $R$, belongs to the noninjectivity range, it will generate two pores. These pores cannot appear simultaneously, but only one of them. With the other words these pores will be competitive pores. Although, they are geometrically different, the probability of appearance of any of them is the same. If the pertubation radius, $R$, belongs to the bijection range, then only a single pore can appear.

The two sub-ranges of CR may be divided depending on the nature of the pore states. The pores may be closed, open and stable, or open and unstable.

## 3.5. Influence of hydrophobic core thickness on transbilayer pores appearance

The bilayer hydrophobic thickness is determined both by the length and tilt of the phospholipid chains. To examine the influence of hydrophobic core thickness we have chosen five lipid bilayers with the following hydrophobic core thickness ($2h$): 21.7, 23, 24.5, 28.5 and 30.5 Å. We considered that the most part of bilayer thickness fluctuation is given by the hydrophobic thickness fluctuation. The other parameters have the same values for all chosen bilayers: $a_0$ = 38.6 Å$^2$, $T$ = 300 K, $\overline{B}$ = $5\cdot10^7$ N/m, $K_1$ = $0.933\cdot10^{-11}$ N, and $\gamma$ = $15\cdot10^{-4}$ N/m [27].

The results obtained for the radius of the perturbed region $R$, the BLM deformation wavelength ($\lambda$), and the pore radius are plotted in Fig. 4. We can see that for the first three lipid bilayers, the BLM deformation wavelength $\lambda$ is one-to-one function on the perturbation domain radius ($R$), whereas for the other two is not one-to-one function. This means that, there is a lipid bilayer with

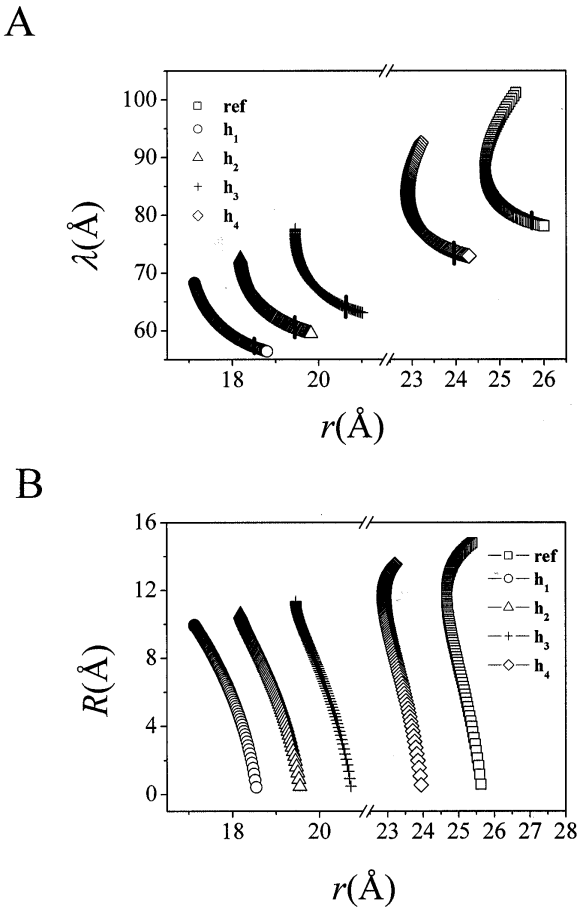


**Figure 4.** BLM deformation wavelength versus pore radius (A), and the perturbation domain radius versus pore radius (B) for membranes with different hydrophobic thicknesses. Curves marked by (□) are indicated for the reference BLM, which has the hydrophobic thickness $2h$ = 30.5 Å. Curves marked by (o), (△), (+) and (◊) are indicated for BLMs with the hydrophobic thickness of 21.7, 23.0, 24.5 and 28.5 Å, respectively. The region from each plot located at lower branch end (indicated by scattered graph) of panel (A) corresponds to closed transbilayer pores. Other BLM parameters are equal to the values of the reference BLM ($a_0$ =38.6 Å$^2$, $T$ = 300 K, $\overline{B}$ = 5×10$^7$ Nm$^{-2}$, $K_1$ = 0.93×10$^{-11}$ N, $\gamma$ = 15×10$^{-4}$ Nm$^{-1}$).

hydrophobic thickness $h_0$ (which is approximately, $2h_0 \approx 28$ Å) that separates lipid bilayers in two categories: (i) lipid bilayers with $h \le h_0$, that we shall call *thin lipid bilayers*, in which is possible to appear a single pore that may be open, or resealed. Both types of pores are stable. For these bilayers, the most probable pore is the narrowest pore, which has the radius $r$ = 10 Å; (ii) lipid bilayers with $h \ge h_0$, that we shall call *thick lipid bilayers*. For these bilayers, their CR must be divided in two sub-ranges: uninjectivity range and bijection range.

For perturbation radius $R$ from uninjectivity range, iso-energetical pores are possible: one of them is larger and the other is narrower than the most probable

pore. For example, for lipid bilayer with hydrophobic thickness $2h$ = 30.5 Å, the larger pore has the radius 11.7 Å ≤ $r_p$ = 14.8 Å, while the corresponding narrow pore has the radius 3.4 Å ≤ $r_p$ = 11.7 Å. The radius of the most probable pore increases from 10 Å for $2h$ = 21.7 Å to 11.7 Å for $2h$ = 30.5 Å, but one seems to reach rapidly o constant value of about 11.7 Å for bilayers thicker than $2h_0$.

The maximum pore radius increases with increasing hydrophobic core thickness. However, for all cases examined here the largest pore remains smaller than the critical pore ($rc \approx h$), so that the pores that form in the lipid bilayer due to thermal movements are stable. For example, for $2h$ = 21.7 Å, we can get $r$ = 10 Å, and for $2h$ = 30.5 Å, we can obtain $r$ = 14.8 Å. The perturbation radius, and implicitly the number of lipid molecules participating in a thermal group motion increases. For lipid bilayers with $2h$ = 21.7 Å, the CR is [17.1 – 18.8] Å, while for lipid bilayers with $2h$ = 30.5 Å, this range shifts to higher values of [24.7 – 26.0] Å. The width of the CR decreases.

A lipid bilayer does not have perfectly planar surfaces, because lipid regions within cell membranes are lipid mixtures, and lipids associate selectively depending on the hydrophobic chain lengths. In other terms, the cases already analyzed here can coexist in the same BLM.

## 3.6. Influence of the polar headgroup size

The polar headgroup size is characterized by the area occupied by a single phospholipid on the lipid bilayer surface. For planar lipid bilayers, this area is equal to the cross-section area of the polar group. The actual area occupied by a single molecule on the bilayer surface depends on the polar headgroup size, its degree of hydration, the hydrophobic chain length and the temperature. For the unhydrated lipid bilayers, we have $a_0$ = 38.6 Å$^2$ [52]. In this work, we have considered four planar lipid bilayers constituted of lipids with the polar headgroups: 38.6 Å$^2$, 45 Å$^2$, 50 Å$^2$ and 60 Å$^2$. The hydrophobic core thickness for all four bilayers is equal to 30.5 Å. The results are plotted in Fig. 5. The direct effect of the increasing cross-sectional area of the polar headgroups is the increase of the minimum value of the perturbed region radius R0, but the number of lipid molecules, which participate to the collective thermal motion does not increase substantially. Therefore, the probability of appearance of the most probable pore decreases with increasing cross-sectional area of the polar headgroup.

The cross-sectional area increase has three important effects:

(i) the radius of the most probable pore decreases from 11.7 Å for $a_0$ = 38.6 Å$^2$ to 8.1 Å for $a_0$ = 60 Å$^2$;

(ii) the formation of unstable pores. The hydrophobic core thickness of all lipid bilayers studied in this section is 2h = 30.5 Å, so that the critical radius is $r_c \approx h$ =15.25 Å. The increase of cross-sectional area of polar headgroup favors

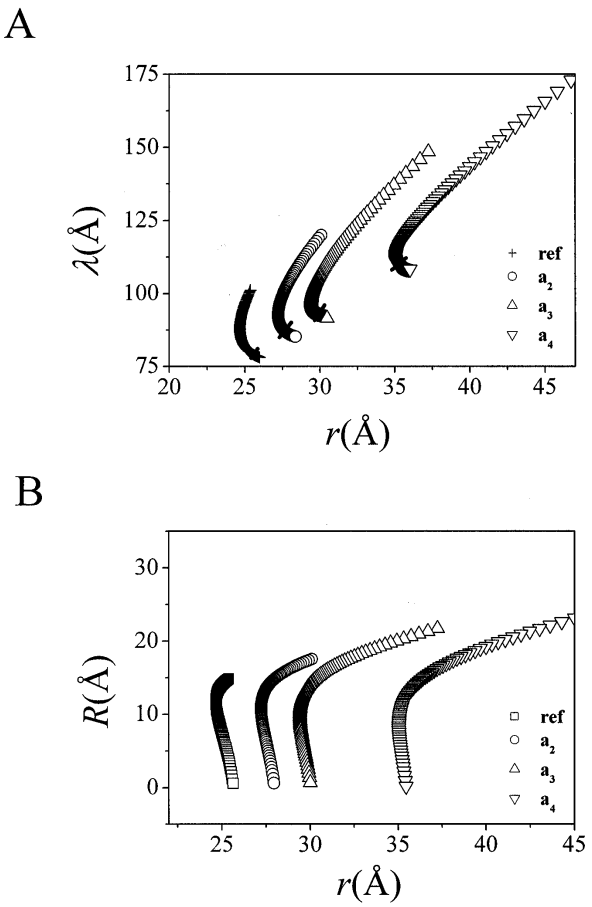


**Figure 5.** BLM deformation wavelength versus pore radius (A), and the perturbation domain radius versus pore radius (B) for membranes containing phospholipids with different polar headgroup sizes. Curves marked by (+) are indicated for the reference BLM, which is consisted of phospholipids with a cross-sectional area $a_o$ = 38.6 Å$^2$. Curves marked by (○), (△) and (∇) are denoted for BLMs containing phopholipids with a cross-sectional area of 45, 50 and 60 Å$^2$, respectively. The region from each plot situated at lower branch end (indicated by scattered graph) of panel (A) corresponds to closed transbilayer pores. Other BLM parameters are equal to the values of the reference BLM ($2h$ =30.5 Å, $T$ = 300 K, $\overline{B}$ = 5×10$^7$ Nm$^{-2}$, $K_1$ = 0.93×10$^{-11}$ N, γ = 15×10$^{-4}$ Nm$^{-1}$).

large BLM deformation wavelength, so that the formation of larger pores rather than the most probable pore (Fig. 5). For lipid bilayers containing molecules with cross-sectional area larger than 45 Å$^2$, pores with a radius larger than critical radius $r_c$ are possible. These pores evolve to membrane rupture;

(iii) the diversification of combinations of pore states, which can be generated by thermal motion [27].

It is obvious that the size of the perturbation area, expressed by the radius R, will increase significantly with the increase of the cross-sectional area of the polar headgroup. A more realistic parameter to characterize lipid bilayer perturbation is the number of molecules involved in thermal group motion

(because they possess the thermal energy necessary for lipid bilayer deformation).

For a clearer presentation of the results concerning the influence of the polar headgroup size on transbilayer pore formation, we can look at Fig. 5. The compatibility range was divided in three sub-ranges. The results obtained for $R$, $\lambda$, and $r$ were organized in ascending order of the perturbation radius $R$. For the first range, $R_0 - R_1$, $\lambda = \lambda(R)$ and $r = r(R)$ are not one-to-one functions of $R$. For each $R$ value in the sub-range ($R_0$, $R_1$) corresponds two values of $\lambda$ and $r$, respectively. For lipid bilayers with $a_0 = 38.6$ Å$^2$, the first $R$ sub-range is $R_0 - R_1$ = [24.7 – 25.4] Å. For each value of R belonging to this sub-range corresponds two values of $\lambda$ from sub-ranges: $\lambda_0 - \lambda_{1t}$ = [87.9 – 101.6] Å (t -top branch) and $\lambda_0 - \lambda_{1b}$ = [87. – 79.8] Å, (b-bottom branch) and two values of $r$ (pore radius) sub-ranges: $r_0 - r_{1l}$ = [11.7– 14.8] Å (large pore) and $r_0 - r_{1n}$ = [11.7 – 4.0] Å (narrow pore).

We can notice that, for larger values of the polar headgroup size, the BLM deformation wavelengths are favored, while the probability of lipid bilayer breakdown by thermally induced fluctuations decreases. The simultaneous displacement of 50 – 59 molecules is enough to generate a stable pore. For unstable pores, a rapid increase of the number of phospholipids can be noticed: $N \in$ [59 – 87] for $a_0 = 50$ Å$^2$, and $N \in$ [69 – 152] for $a_0 = 60$ Å$^2$.

## 3.7. The influence of temperature

In this review article, the thermally induced movement of molecules is the energy source for lipid bilayer deformation, which ultimately results in the formation of transbilayer pores. Therefore, temperature is an external factor with direct influence on pore occurrence. We have considered the lipid bilayers with temperatures of 300 K, 310 K, and 320 K, all located below the phase transition temperature (Fig. 6). We expect the perturbation size and the number of molecules involved in pore-forming thermal group motion to decrease with a temperature increase. Calculation of deformation energy, according to the elastic theory of continuous media applied to type A smectic liquid crystals, permitted the study of pore formation for any planar lipid bilayer, provided that the parameters of equation (1) are known. In the present work we wanted to examine the influence of hydrophobic core thickness, polar group size and temperature. At temperatures below the phase transition temperature, for thin bilayers ($2h < 28$ Å), a single stable open pore of radius $r < 11$ Å or a closed pores could be formed. Surprisingly, out of this list of parameters, the temperature exerts the weakest influence. This result is very important, if we consider pathological conditions that may be accompanied by unstable pore formation, and result in cell destruction due to lipid membrane rupture.

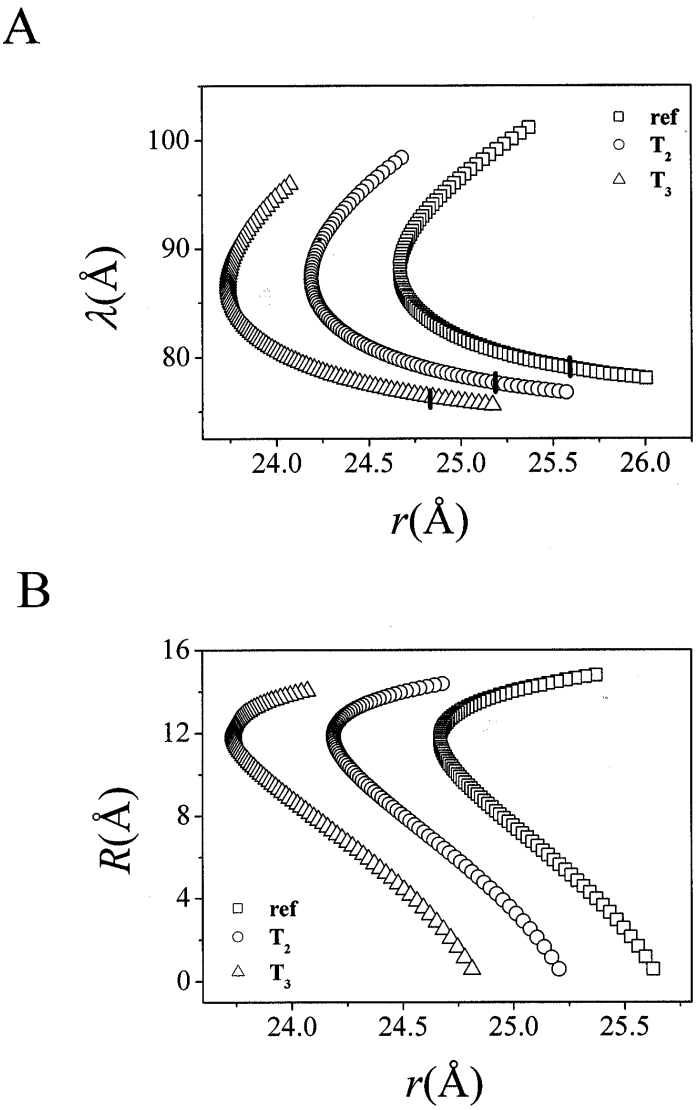


**Figure 6.** BLM deformation wavelength versus pore radius (A), and the perturbation domain radius versus pore radius (B) for membranes with different temperatures. Curves marked by (□) are indicated for the BLM with a temperature of 300 K. Curves marked by (o) and (Δ) are indicated for BLMs for which the temperature is 310 and 320 K, respectively. The region from each plot located at lower branch end (indicated by scattered graph) of panel (A) corresponds to closed transbilayer pores. Other BLM parameters are equal to the values of the reference BLM ($2h$ =30.5 Å, $\overline{B} = 5\times10^{7}$ Nm$^{-2}$, $K_1 = 0.93\times10^{-11}$ N, $\gamma = 15\times10^{-4}$ Nm$^{-1}$).

Although the radius of the pore increases with increasing hydrophobic core thickness, it will always exhibit lower values than the BLM half-thickness. At larger values of hydrophobic core thickness, two pores can occur with equal probability, one larger than the other, but the BLM stability is not affected. The most troublesome effect is given by the polar headgroup size, because larger values of this parameter can lead to unstable pores evolving to bilayer rupture.

The polar headgroup size exerts a substantial effect due to the hydration of the BLM polar headgroup regions. Unstable pores have a very low probability of occurrence, because the necessary BLM deformation energy is high.

Very recently, Fournier and Joos (2003) [16] developed a model for the kinetics of rupture of fluid bilayer membrane. The pore formation was considered as a thermally activated process. The model included the physical properties of the fluid lipid bilayer as a result of the hydrophobility of the hydrocarbonic chains. The membrane was characterized by the bulk compressibility $K$, the bilayer thickness $2h$ of the hydrophobic part as well as a parameter $\gamma$ indicating the chain rigidity of the phospholipids. The parameter $\gamma$ was used to examine the effect of the saturation of the phospholipid chains on the structural traits of the fluid lipid bilayer. Therefore, both the nucleation and growth of the pores were explained in terms of the hydrophobic forces, which are responsible for the line energy and the bulk conductivity.

# 4. Transbilayer pores induced by electric fields

Transient pores in lipid membranes may also be generated by electric fields [8]. In other situations, the electric field opposes the pore opening or even stabilizes the pores of a certain size [53,54]. If a membrane is exposed to a high transmembrane potential, it may experience a rapid increase in electrical conductivity by several orders of magnitude [6,7,10]. Such a drastic modification of the barrier function is caused by proliferation of the electrically induced transmebrane pores that represent the translocation pathways for water and electrolytes across the lipid bilayer.

It was hypothesized that for certain transmembrane potentials, higher than 200 mV, the transbilayers pores have a radius of at least 10 Å [55,56]. Neu and co-workers (2003) [11] calculated the contribution of externally induced transmembrane potential to the free energy of large and highly conductive transbilayer pores. The formalism used for this calculation employed the formula for mechanical work that is required to deform a dielectric body, immersed in ionic solution, with a constant electric current. The formula for the energy of a cylindrical or a toroidal pore (Fig. 7) demonstrated a linearity increase for pore radii larger than 20 nm [11]. These calculations are important for a better understanding of the electrical energy of large pores in order to rationalize the electrical pulsing protocols for the DNA injection into the cells. Entropy is a dominant factor for the pore growth when the line tensions are comparable with those measured for artificial vesicles.

Sung and Park (1997) [20,21] used statistical physics of non-Markovian stochastic process over a free energy barrier to derive an analytical form of the lifetime of a metastable pore in a membrane. This calculation permitted the assessment of the phase diagram for the stability of the transbilayer pore and its

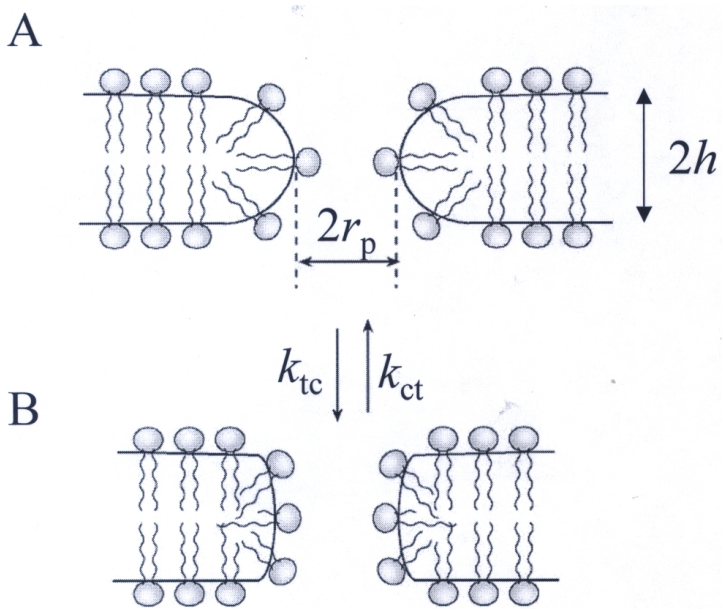


**Figure 7.** Pore models for electroporation with (A) cylindrical and (B) toroidal geometry of their inner surface. A transition of the pore geometry from cylindrical to toroidal or vice-versa is hypothesized, with a nonlinear dependence on the local transmembrane voltage [11,12,10].

dependence on the membrane and environmental parameters. Very recently, Neu and Krassowska (2003) [12] examined the evolution of large electrically induced pores by numerical simulations of the Smoluchowsky equation. As expectedly after the electrical shock, the transbilayers pores, depending on their cross-sectional radius, either shrink to zero-radius pores or expounds until to the rupture of the bilayer membrane. The timescale of these processes measure about one microsecond or less. Benz and his co-workers [54] studied the kinetics of pore opening and evolution to mechanical rupture of lipid bilayer membranes using the charge-pulse method. The characteristic opening process was independent of the transmembrane potential and electrolyte concentration. According to theoretical interpretation of these experiments, the voltage-induced irreversible breakdown of the membranes is caused by a decrease in boundary (edge) energy of the pore. Upon initiation of the pore formation, the electrical influence on the surface tension is marginal. The novelty of this work consisted in the idea that the transmembrane potential has a negligible contribution on the conductance increase during the mechanical breakdown upon the pore formation. This is because the electrical field promotes a decrease in free energy barrier for the transbilayer pore formation. Therefore, increasing the transmembrane potential will increase the number of pores, but without changing the kinetics of pore opening. The pore resealing after electroporation of a cell membrane was also studied by Saulis (1997) [9]. Two distinct situations were studied: (i) the rate of pore formation was comparable with the

rate of the pore resealing, and (ii) the rate of pore formation is significantly lower than the rate of pore resealing. In the former case, a steady state number of pores in the cell membrane was noticed. In the latter case, the pores disappear completely. The pore resealing was modelled by Saulis (1997) as a multi-step and stochastic process [9].

# 5. Molecular dynamics simulations of a transient or a stable pore in a membrane

Berendsen and co-workers used the molecular dynamics simulations to examine the proton transport across the hydrophobic environment of a phospholipid membrane [48]. The probability of the transbilayer pore appearance was calculated from the free energy landscape associated with the necessary force to induce a single water pore into a membrane. The lifetime of a single file of waters spanning the bilayer, requiring a free energy of about 100 kJ/mol, was in a picosecond timescale, thus demonstrating the transient nature of the pore. The dynamics of the defects in the membrane as well their translocation from one monolayer to the other was also observed. The fast proton diffusion across a single water pore, when the waters undergo a suitable orientation, was postulated by a wire-like conductance mechanism. Membrane rupture was studied by a newly proposed technique of dissipative particle dynamics, in which several atoms are united in a single simulation particle [57]. Three carbon atoms or water molecules were represented by a simulation particle. This simplification of the system allowed an increase of up to five orders of magnitude in computational speed. The transient and stable water pores were found to vary with the composition of mixed bilayers between lipids and non-ionic surfactants. Recently, Marrink and collaborators have used molecular dynamics simulations to detect, at an atomic level, the transient pore formation in a bilayer consisting of 128 lipids and 6029 water molecules [13]. Both mechanical, with a lateral pressure higher than –200 bar, and electrical stress, with a field intensity of 0.5 V/nm were studied. The rupture of the bilayer, which is initiated in 4-12 ns timescale, develops rapidly, thus forming a cylindrical pore. The pore is highly unstable, its size increasing until the bilayer is broken. In contrast, an electric field induces a population of local defects. The water molecules partition the bilayer hydrophobic core due to these local defects. In an intense electric field, the waters are strongly oriented, therefore the membranes pores form with marginal change in surface area. The headgroups of the phospholipids are also aligned with the external electric field. The molecular dynamics simulations revealed similarities and differences in behavior of lipids and waters, depending on whether the pore is brought about by an external electric field or by mechanical stress. In both cases, Marrink and collaborators [13] found that the pore is initiated through *single file defects*,

which are chains of waters that span the thickness of the bilayer from one monolayer to the other.

The metastable transmembrane pore was observed during the molecular dynamics simulations of the spontaneous aggregation of phospholipids into bilayers [17]. Self-assembling of phopsholipids to form ordered bilayer systems is a fundamental process in membrane biology. Marrink et al. (2001) [17] observed the self-aggregation of the lipids at atomic detail starting from random solutions. The metastable transmembrane pore can be probed as an intermediate state during the transition from an isotropic liquid of randomly oriented phospholipids to an ordered bilayer system. The initiation of the pore revealed a wide hole with about 100 dissolved waters followed by a relaxation process with final metastable structure of 1 to 1.5 nm in diameter, which includes about 50 waters. The headgroup conformational, reorientation and hydration changes during the pore lifetime are accompanied by substantial free energy barrier.

# 6. Passive flip-flop diffusion of lipids across transbilayer pores

Phospholipids can translocate passively from one monolayer to the other [2,15,40,58]. This transversal diffusion is basically caused by their perpendicular oscillations on the bilayer surface as well as the local defects of the membrane. The stochastic pores brought about by self-oscillations of the bilayer membrane might represent a driving way for the passive flip-flop diffusion of phospholipids. The appearance of statistical pores through lipid membranes due to the self-oscillations of the membrane is associated with the presence of three energetic barriers: perforation of the membrane, with the energy height $\Delta W_1$; recovery of the membrane, with the energy height $\Delta W_2$; breaking of the membrane, with the energy height $\Delta W_3$.

The membrane can be found in one of the following three states [59]: state 1, which assumes the absence of the transmembrane pores, namely in the phase preceding the pore formation; state 2, which is associated with a single transmembrane pore, regardless the diameter of the pore; and state 3, which is associated with the breakdown of the membrane.

The kinetics of state transitions of the membrane is the following:

$$1 \underset{k_2}{\overset{k_1}{\rightleftarrows}} 2 \xrightarrow{k_3} 3 \tag{13}$$

with the rates:

$$k_1 \approx \exp(-\beta \Delta W_1) \tag{14}$$

$$k_2 \approx \exp(-\beta \Delta W_2) \tag{15}$$

$$k_3 \approx \exp(-\beta \Delta W_3) \tag{16}$$

where $\beta = 1/k_B T$ has usual meaning.

If we denote the probabilities that at a given time the membrane is found to be in the states 1, 2 and 3, by $P_1(t)$, $P_2(t)$ and $P_3(t)$, respectively, then the kinetic scheme of the system is given by:

$$dP_1 / dt = k_2 P_2(t) - k_1 P_1(t) \tag{17}$$

$$dP_3 / dt = k_3 P_2(t) \tag{18}$$

$$P_1(t) + P_2(t) + P_3(t) = 1 \tag{19}$$

with the initial conditions: $P_1(0) = 1$, $P_2(0) = 0$, $P_3(0) = 0$.

If we introduce a dimensionless rate variable defined by the following expression:

$$\tau = (k_1 + k_2 + k_3)t \tag{20}$$

Then, the probabilities for each of the three states are given by:

$$P_1 = [(x_1 + v)\exp(x_2 \tau) - (x_2 + v)\exp(x_1 \tau)] / y \tag{21}$$

$$P_2 = v[\exp(x_1 \tau) - \exp(x_2 \tau)] / y \tag{22}$$

$$P_3 = 1 - [x_1 \exp(x_2 \tau) - x_2 \exp(x_1 \tau)] / y \tag{23}$$

where the auxiliary relations:

$$v = k_1 (k_1 + k_2 + k_3)^{-1} \tag{24}$$

$$u = k_1 k_2 (k_1 + k_2 + k_3)^{-2} \tag{25}$$

$$y = \sqrt{1 - 4u} \tag{26}$$

$$x_1 = (y-1)/2 \tag{27}$$

$$x_2 = -(y+1)/2 \tag{28}$$

The distribution function of the lifetime of the transbilayer pore is:

$$F(\tau) = P_3(\tau) \tag{29}$$

Therefore, the probability density is given by:

$$f(\tau) = dF(\tau)/d\tau = u\exp(x_1\tau)[1-\exp(-y\tau)]/y \tag{30}$$

Finally, the mean lifetime $\overline{\tau}$ of the transbilayer pore is:

$$\overline{\tau} = \int_0^\infty \tau f(\tau) d\tau = 1/u \tag{31}$$

The mean number of pores $\overline{n}$ is equal to the probability of a pore appeared on a stable membrane [26]:

$$\overline{n} = P_2/(P_1+P_2) = v[\exp(y\tau)-1]/x_1 \tag{32}$$

The number of phospholipids across the median plane of the lipid bilayer neighboring statistical pores is equal to:

$$dN_{ff} = ndN_t \tag{33}$$

where $dN_t$ is the number of molecules that undergo a translocation through the pore. Therefore, the flip-flop diffusion coefficient is $D_{ff} = nD_l$.

We can have an estimate of $n$:

$$n \approx k_1/(k_1+k_2+k_3) \tag{34}$$

From the calculation presented in reference Popescu et al. [29], we obtain the free energy barriers for $\Delta W_1$, $\Delta W_2$ and $\Delta W_3$ (91.2, 65.6 and 2,090 $k_BT$, respectively) [59]. Then it was obtained $n = exp(-25)$. Because the lateral diffusion coefficient ($D_l$), of the phospholipids at the surface of the planar bilayer is in the order $10^{-12}$ $m^2s^{-1}$, this gives the value $D_{ff} = 10^{-12}exp(-25) = 10^{-23}$ $m^2s^{-1}$.

If we consider a lipid bilayer with a thickness of 30 Å, then the translocation time $\tau$ is the following:

$$\tau = \overline{r^2} / D_{ff} = 2.25 \times 10^5 \text{ s} \quad (35)$$

It is interesting that this is in the same order of magnitude as the lifetime of other phospholipids in a lipid bilayer. This simple calculation demonstrates that the passive flip-flop translocation of phospholipids through a metastable pore formed in a lipid bilayer is a very rare, but detectable event [40,59].

# 7. Summary

Undoubtedly, the presence of hydrophilic pores in equilibrium membranes is of fundamental importance in biomedical sciences. Under mechanical, thermal, osmotic and electrocompressive stress, such metastable transmembrane pores can become stable, thus inducing finally the rupture of the entire membrane. The stochastic pores in membranes may also represent intermediate states in phase transitions, membrane fusion and budding. In addition, the electroporation and fusion of electroporated cells determine novel biotechnological applications such as drug delivery and gene therapy.

# Acknowledgments

The stimulating discussions with Constantin Fetecau, Ion Stelian and Beatrice Macri are highly appreciated. LM would like to thank Syracuse University for the Start-up Funds.

# References

1. Sackmann, E. 1995, Biological membranes: architecture and function, Elsevier/North-Holland.
2. Holthuis, J. C. M., van Meer, G., and Huitema, K. 2003, Mol. Membrane Biol., 20, 231.
3. Humpert, C. and Baumann, M. 2003, Mol. Membrane Biol., 20, 155.
4. May, S. 2000, Curr. Op. Colloid & Interface Sci., 5, 244.
5. Kessel, A., Ben Tal, N., and May, S. 2001, Biophys. J., 81, 643.
6. Bordi, F., Cametti, C., and Motta, A. 2000, J. of Phys. Chem. B, 104, 5318.
7. Bordi, F., Cametti, C., and Naglieri, A. 1999, Colloids and Surfaces A-Physicochem. and Eng. Aspects, 159, 231.
8. Freeman, S. A., Wang, M. A., and Weaver, J. C. 1994, Biophys. J., 67, 42.
9. Saulis, G. 1997, Biophys. J., 73, 1299.
10. Neu, J. C. and Krassowska, W. 1999, Phys. Rev. E, 59, 3471.
11. Neu, J. C., Smith, K. C., and Krassowska, W. 2003, Bioelectrochem., 60, 107.
12. Neu, J. C. and Krassowska, W. 2003, Phys. Rev. E, 67,

13. Tieleman, D. P., Leontiadou, H., Mark, A. E., and Marrink, S. J. 2003, J. Amer. Chem. Soc., 125, 6382.
14. Shillcock, J. C. and Seifert, U. 1998, Biophys. J., 74, 1754.
15. Farago, O. 2003, J. Chem. Phys., 119, 596.
16. Fournier, L. and Joos, B. 2003, Phys. Rev. E, 67,
17. Marrink, S. J., Lindahl, E., Edholm, O., and Mark, A. E. 2001, J. Amer. Chem. Soc., 123, 8638.
18. Shillcock, J. C. and Boal, D. H. 1996, Biophys. J., 71, 317.
19. Moroz, J. D. and Nelson, P. 1997, Biophys. J., 72, 2211.
20. Sung, W. and Park, P. J. 1997, Biophys. J., 73, 1797.
21. Sung, W. Y. and Park, P. J. 1998, Physica A, 254, 62.
22. Karatekin, E., Sandre, O., Guitouni, H., Borghi, N., Puech, P. H., and Brochard-Wyart, F. 2003, Biophys. J., 84, 1734.
23. Zhelev, D. V. and Needham, D. 1993, Biochim. Biophys. Acta, 1147, 89.
24. Litster, J. D. 1975, Phys. Letters A, A 53, 193.
25. May, S. 2000, Eur. Phys. J. E, 3, 37.
26. Popescu, D. and Margineanu, D. G. 1981, Bioelectrochem. & Bioenerg., 8, 581.
27. Popescu, D., Ion, S., Popescu, A. I., and Movileanu, L. 2003, Planar Lipid Bilayers (BLMs) and Their Applications, H. Ti Tien and A. Ottova (Eds.), Elsevier Science Publishers, Amsterdam, 173.
28. Karatekin, E., Sandre, O., and Brochard-Wyart, F. 2003, Polymer Int., 52, 486.
29. Popescu, D., Rucareanu, C., and Victor, G. 1991, Bioelectrochem. & Bioenerg., 25, 91.
30. Brochard-Wyart, F., de Gennes, P. G., and Sandre, O. 2000, Physica A, 278, 32.
31. Sandre, O., Moreaux, L., and Brochard-Wyart, F. 1999, Proc. Natl. Acad. Sci. USA, 96, 10591.
32. Boal, D. H. 2001, Mechanics of the Cell, Cambridge University Press, Cambridge.
33. Benz, R., Frohlich, O., Lauger, P., and Montal, M. 1975, Biochim. Biophys. Acta, 394, 323.
34. Hladky, S. B. and Gruen, D. W. R. 1984, Biophys. J., 45, 645.
35. Hladky, S. B. and Gruen, D. W. R. 1982, Biophys. J., 38, 251.
36. Popescu, D. 1993, Biochim. Biophys. Acta, 1152, 35.
37. Movileanu, L. and Popescu, D. 1995, Biosystems, 36, 43.
38. Movileanu, L. and Popescu, D. 1996, J. Biol. Systems, 4, 425.
39. Popescu, D. and Victor, G. 1990, Biochim. Biophys. Acta, 1030, 238.
40. Movileanu, L., Popescu, D., Victor, G., and Turcu, G. 1997, Biosystems, 40, 263.
41. Movileanu, L., Popescu, D., and Flonta, M. L. 1998, Theochem-J. Mol. Struct., 434, 213.
42. Movileanu, L. and Popescu, D. 1998, Acta Biotheor., 46, 347.
43. Huang, H. W. 1986, Biophys. J., 50, 1061.
44. Helfrich, P. and Jakobsson, E. 1990, Biophys. J., 57, 1075.
45. Nielsen, C., Goulian, M., and Andersen, O. S. 1998, Biophys. J., 74, 1966.
46. Nielsen, C. and Andersen, O. S. 2000, Biophys. J., 79, 2583.
47. May, S. 2000, Eur. Biophys. J. Biophys. Letters, 29, 17.
48. Marrink, S. J., Jahnig, F., and Berendsen, H. J. C. 1996, Biophys. J., 71, 632.
49. De Gennes, P.-G. 1974, The Physics of Liquid Crystals, Clarendon Press, Oxford.

50. Rawicz, W., Olbrich, K. C., McIntosh, T., Needham, D., and Evans, E. 2000, Biophys. J., 79, 328.
51. Popescu, D and Rucareanu, C. 1992, Mol. Cryst. Liq. Cryst., 25, 339.
52. Popescu, D. and Victor, G. 1991, Biophys. Chem., 39, 283.
53. Winterhalter, M. and Helfrich, W. 1987, Phys. Rev. A, 36, 5874.
54. Wilhelm, C., Winterhalter, M., Zimmermann, U., and Benz, R. 1993, Biophys. J., 64, 121.
55. Weaver, J. C. 2003, IEEE Trans. Diel. Electrical Ins., 10, 754.
56. Weaver, J. C. 2000, IEEE Trans. Plasma Sci., 28, 24.
57. Groot, R. D. and Rabone, K. L. 2001, Biophys. J., 81, 725.
58. Popescu, D., Movileanu, L., Victor, G., and Turcu, G. 1997, Bull. Math. Biol., 59, 43.
59. Popescu, D. and Victor, G. 1991, Bioelectrochem. & Bioenerg., 25, 105.